



# Ionization of Porous Hypercrosslinked Polymers for Catalyzing Room-Temperature CO<sub>2</sub> Reduction via Formamides Synthesis

Qinggong Ren<sup>1</sup> · Yaju Chen<sup>1</sup> · Yongjian Qiu<sup>1,2</sup> · Leiming Tao<sup>1</sup> · Hongbing Ji<sup>1,2,3</sup>

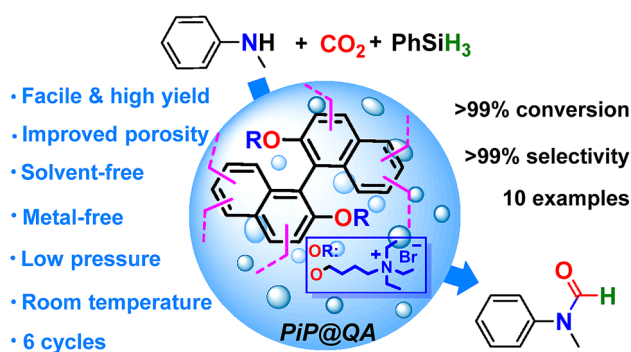
Received: 5 November 2020 / Accepted: 28 December 2020

© The Author(s), under exclusive licence to Springer Science+Business Media, LLC part of Springer Nature 2021

## Abstract

Porous materials with heterogeneous nature occupy a pivotal position in the chemical industry. This work described a facile pre- and post-synthetic approach to modify porous hypercrosslinked polymer with quaternary ammonium bromide, rendering it as efficient catalyst for CO<sub>2</sub> conversion. The as-prepared porous ionic polymer (PiP@QA) displayed an improved specific surface area of 301 m<sup>2</sup>·g<sup>-1</sup> with hierarchically porous structure, good selective adsorption of CO<sub>2</sub>, as well as high ion density. Accordingly, PiP@QA catalyst exhibited excellent catalytic performances for the solvent-free synthesis of various formamides from CO<sub>2</sub>, amines and phenylsilane under 35 °C and 0.5 MPa. We speculated that the superior catalytic efficiency and broad substrate scope of this catalyst could be resulted from the synergistic effect of flexible ionic sites with unique nanoporous channel that might increase the collision probability of reactants and active sites as well as enhance the diffusion of reactants and products during the reaction process. With the good reusability, PiP@QA was also available for the efficient conversion of simulated flue gas (15% CO<sub>2</sub> in N<sub>2</sub>, v/v) into target formamides with quantitative selectivity at room temperature, which further highlighted its industrial application potential in chemical recycling the real-world CO<sub>2</sub> to valuable products.

## Graphic Abstract



**Keywords** Porous ionic polymers · Carbon dioxide · Reduction · N-formylation · Heterogeneous catalysis

## 1 Introduction

Chemical fixation of carbon dioxide (CO<sub>2</sub>) into valuable products has attracted continuous attention in both scientific research and industrial investment, since CO<sub>2</sub> is an abundant, eco-friendly and renewable C1 feedstock [1–3]. Owing to the thermodynamic and/or kinetic barriers in the activation, the functionalization of CO<sub>2</sub> via formation of C–O, C–N,

✉ Yaju Chen  
chenyaju970@126.com

✉ Hongbing Ji  
jihb@mail.sysu.edu.cn

Extended author information available on the last page of the article

C–C or C–H bond under mild conditions especially at room temperature is still a challenging task [4–6]. Recently, the selective reduction of CO<sub>2</sub> with amines in the present of reductants into formamides has regarded as a promising route for carbon cycling because of the application potential of these products in medicines, pesticides, dyes, adhesives, etc. [7].

As a common reductant, molecular hydrogen has been widely applied in the synthesis formamides from CO<sub>2</sub> and amines under harsh reaction conditions (> 100 °C and/or > 5 MPa) [8]. In this regard, the development of mild reaction process to fix CO<sub>2</sub> to formamides is highly attractive. Fortunately, organosilanes have been well documented to achieve this transformation under mild conditions. Up to now, numerous catalysts such as metal salts [9–11], metal complexes [11, 12], N-heterocyclic carbenes [7, 13], phosphorus ylides [14, 15] and ionic liquids (ILs) [14, 16], have been developed for this N-formylation reaction. Among these, ILs presented distinct advantages of sustainability, stability and high efficiency. For example, Yang and coworkers [16] reported a series of eco-friendly acetylcholine-carboxylate bio-ILs for producing formamides using ambient CO<sub>2</sub> at low temperature. Glycine betaine was developed for the reductive functionalization of CO<sub>2</sub> with amines and organosilanes by He's [17] and Han's [8] groups. Despite significant progress, the presently available ILs-based homogenous catalytic systems mainly suffered from the drawbacks of difficult products purification and costly catalyst separation, recycling, and disposal, thereby limiting their industrial applications. In addition, organic solvents are also required to achieve the catalytic performance [18, 19]. Therefore, the development of heterogeneous ILs-based catalysts for efficient and sustainable N-formylation of amines with CO<sub>2</sub>/organosilanes under ambient conditions is highly desirable.

Porous ionic polymers (PiPs) emerged as a new class of porous materials have been noticed for their high charge density, well-defined porosity, synthetic diversity and CO<sub>2</sub> affinity [20–22]. Hence, PiPs have become a rising star in the area of CO<sub>2</sub> capture and conversion [23–25]. Although

a wide range of chemical reactions and synthetic methods could be directly available to obtain various PiPs, the charge interaction and intermolecular packing in polymerization process led to great decrease of the surface area and porosity [26]. For example, a series of zinc(II) porphyrin-based ionic polymers were synthesized through a one-step and catalyst-free imine condensation reaction [27]. The obtained polymers SYSU-Zn@IL1 and SYSU-Zn@IL2 only gave Brunauer–Emmett–Teller (BET) specific surface areas of 38 and 21 m<sup>2</sup>·g<sup>-1</sup>, respectively. As is known to all, the high surface area is in favor of improving the exposure and accessibility of active sites, and the abundant nanopores are benefit for the enrichment of CO<sub>2</sub> [28, 29]. These features are crucial to achieve the CO<sub>2</sub>-related transformation under mild even ambient conditions.

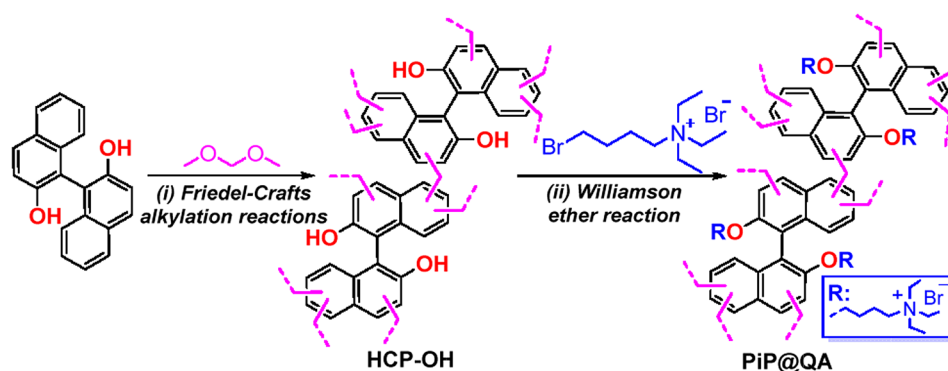
Herein, we presented a pre- and post-synthetic strategy to prepare PiPs with hierarchically porous structure (PiP@QA) based on the Friedel–Crafts alkylation reaction of 1,1'-bi-2-naphthol with formaldehyde dimethyl acetal and subsequent Williamson ether reaction with quaternary ammonium bromide (Scheme 1). The resultant polymer possessed an improved specific surface area, good CO<sub>2</sub>/N<sub>2</sub> selective adsorption and high-density ILs sites. PiP@QA was then employed as efficient heterogeneous catalyst for the solvent-free synthesis of formamides from CO<sub>2</sub>, amines and phenylsilane under ambient reaction conditions. As expected, PiP@QA presented high catalytic efficiency, excellent substrate scope, and good reusability in this transformation even using the diluted CO<sub>2</sub> as a raw material.

## 2 Experimental

### 2.1 Materials

Unless otherwise noted, CO<sub>2</sub> (99.999%) and other chemicals were commercially available from local suppliers and used without further purification. The amines (99%), phenylsilane (PhSiH<sub>3</sub>, 97%) and anhydrous iron(III) chloride

**Scheme 1** Synthesis of porous polymeric catalyst PiP@QA



(98%) were obtained from J&K Scientific Ltd or Alfa Aesar. Formaldehyde dimethyl acetal (FDA), 1,1'-bi-2-naphthol, triethylamine, anhydrous 1,2-dichloroethane and 1,4-dibromobutane with purity over 98% were purchased from Energy Chemical. (2-bromobutyl)triethylammonium bromide ([BrBuNEt<sub>3</sub>]Br, QA) were synthesized according to the literature [30].

## 2.2 Instrumentation

A Bruker Varian INOVA500NB spectrometer was used to record the liquid <sup>1</sup>H and <sup>13</sup>C NMR spectra using TMS as an internal standard. Elemental analysis for C, H, and N was recorded on a Vario EL cube instrument. The bromine content was measured by oxygen flask combustion and mercury nitrate titration technique. Powder X-ray diffraction (PXRD) was performed in the range of  $2\theta = 2.0 \sim 60.0^\circ$  using a Bruker AXS D8 Advanced SWAX diffractometer by depositing powder on glass substrate at 25 °C. Thermogravimetric analysis (TGA) was measured by using a NETZSCH TG 209 F3 Tarsus instrument by heating samples from 30 °C to 800 °C at a heating rate of 10 °C·min<sup>-1</sup> under N<sub>2</sub> atmosphere. X-ray photoelectron spectroscopy (XPS) data were collected on an ESCALAB 250 spectrometer. Scanning electron microscopy (SEM) image was obtained on FEI Quanta 400 FEG. Transmission electron microscopy (TEM) image was obtained on JEM-2100F field emission electron microscope. The N<sub>2</sub> adsorption and desorption isotherm of sample degassed at 130 °C for 12 h under vacuum was measured by using a Micromeritic ASAP2020M analyzer at 77 K. The pore size distribution was analyzed by using nonlocal density functional theory (NLDFT). The CO<sub>2</sub> and N<sub>2</sub> adsorption isotherms were collected from Micromeritic ASAP2020M at 298 K. Gas chromatographic (GC) analysis was performed on a GC2010 gas chromatograph equipped with a flame ionization detector and a capillary column (Rtx-5, 30 m × 0.32 mm × 0.25 μm).

## 2.3 Synthesis of HCP-OH and PiP@QA

Typically, a 100 mL Schlenk flask was charged with 1,1'-bi-2-naphthol (5 mmol, 1.43 g), anhydrous iron(III) chloride (20 mmol, 3.24 g), formaldehyde dimethyl acetal (20 mmol, 1.52 g) and 20 mL anhydrous 1,2-dichloroethane under nitrogen. After stirred at room temperature for 15 min, the reaction mixture was allowed to heat at 80 °C for 24 h. Then, the resulting black solid mixture was cooled to room temperature and added to a 20 mL methanol. The precipitate was filtered and washed repeatedly with water, methanol, THF and acetone, respectively. Subsequently, the polymer was further purified by Soxhlet extractions for 24 h

with methanol. Finally, the desired product (HCP-OH) was obtained as a black powder by dried at 60 °C under vacuum for overnight. Yield: 98%. Elemental analysis: C: 82.76%, H: 11.09%.

To the 25 mL Schlenk flask, as-prepared HCP-OH (300 mg) and K<sub>2</sub>CO<sub>3</sub> (3 mmol, 414 mg) were added into a solution of [BrBuNEt<sub>3</sub>]Br (QA, 2 mmol, 634 mg) in dry DMF (15 mL). The mixture was refluxed in an oil bath under an inert atmosphere for 24 h. After cooling to room temperature, the precipitate was filtered and washed with ethanol, acetone and water, respectively. After freezing drying, the polymer sample (PiP@QA) was obtained in a yield of 94%. Elemental analysis: C 67.58%, H 10.47%, N 2.65%, Br 15.13%.

## 2.4 General Procedures for N-Formylation of N-Methylaniline with CO<sub>2</sub> and PhSiH<sub>3</sub>

To a 10 mL stainless steel autoclave, *N*-methylaniline, PhSiH<sub>3</sub> and catalyst were added quickly. After sealing and purging with CO<sub>2</sub> for 3 times, the autoclave was pressurized with CO<sub>2</sub> to a setting pressure. The reactor was then stirred at 35 °C for a requested time. Subsequently, the excess of CO<sub>2</sub> was vented out slowly, followed by adding ethyl ether (5 mL). The solid catalyst was separated by filtration and the products in the filtrate were analyzed by GC through the internal standard method to obtain the conversion and selectivity. The purity and structure of product (*N*-methyl-*N*-phenylformamide) were also confirmed by <sup>1</sup>H NMR and <sup>13</sup>C NMR spectra. Recyclability tests were carried out by directly using the recovered catalyst that recycled through filtering, washing and drying. Three parallel experiments were carried out, and the conversion and selectivity were taken as the average.

## 3 Results and Discussion

### 3.1 Catalysts Synthesis

The synthetic route of PiP@QA was outlined in Scheme 1. First, the hydroxy-containing hyper-crosslinked polymer (HCP-OH) was synthesized via Friedel–Crafts alkylation reaction. This polyreaction has been extensively documented to obtain highly cross-linked polymeric matrix with high specific surface area and abundant nanopores. Also, this polyreaction have great advantages of high efficiency, convenience and high yield. The multi-hydroxyl groups have high reactivity that can be easily modified with target active sites. As quaternary ammonium salts are high active towards the N-formylation reaction of amines with and CO<sub>2</sub> and organosilanes, the hydroxyl groups were substitution with quaternary ammonium bromide by

Williamson ether reaction. This synthetic approach offers several distinct benefits: (1) avoiding the charge interaction and intermolecular packing in the direct polymerization of charged monomers by post-immobilization of ionic moieties into charge-neutral skeleton with high surface area and abundant porosity; (2) giving an improved PiPs with high charge density and improved surface area; (3) enhancing the CO<sub>2</sub>-philicity and of polymeric framework to enrich CO<sub>2</sub> molecules near the active sites; and (4) increasing the exposure of active site and diffusion of reactants and products..

### 3.2 Catalysts Characterization

The as-prepared polymeric catalysts were insoluble in water, common polar and nonpolar organic solvents, such as DMF, MeOH, THF, and CH<sub>2</sub>Cl<sub>2</sub>. Then, elemental analysis revealed the C, H content of HCP-OH, and C, H, N, Br content of PiP@QA, respectively, which were listed in the “Experimental section”. The chemical composition of HCP-OH and PiP@QA were further examined by XPS analysis

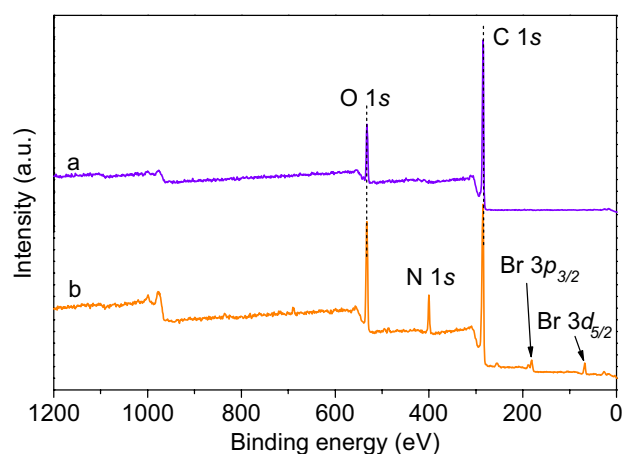


**Fig. 1** XPS spectra of HCP-OH (a) and PiP@QA (b)

**Fig. 2** a Sorption isotherms of nitrogen at 77 K and b pore size distribution diagrams (based on NLDFT method)

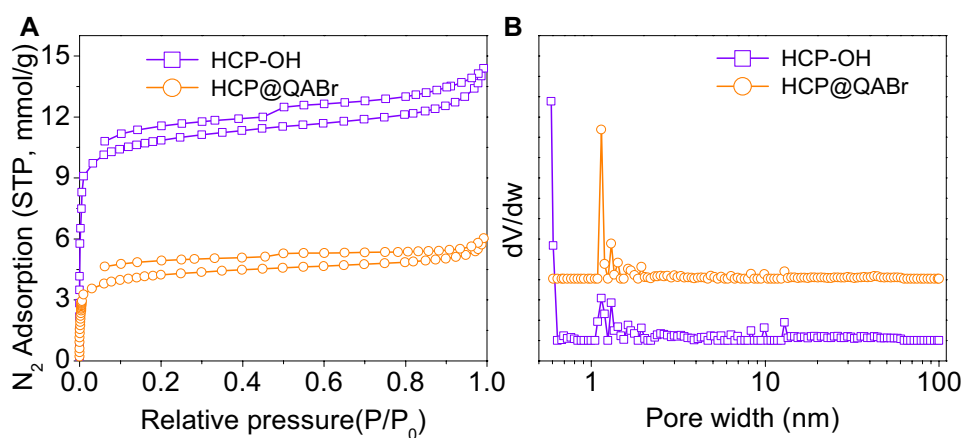


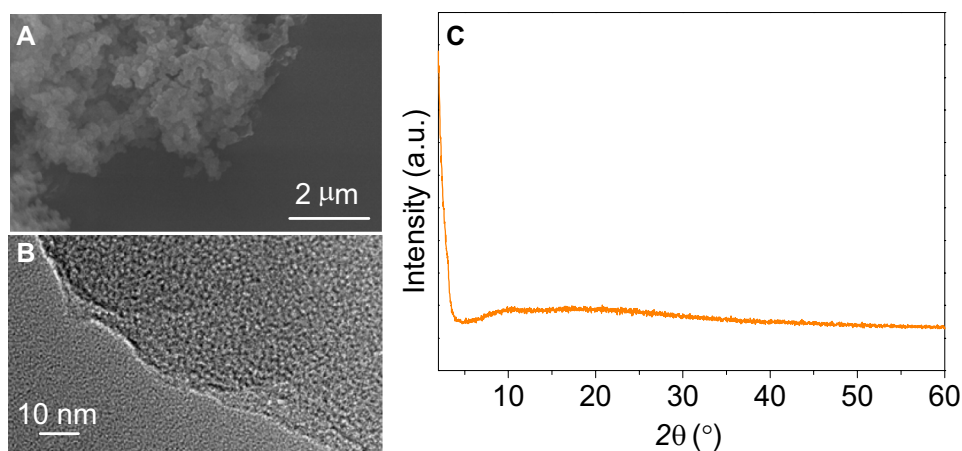
(Fig. 1). As shown in their XPS full spectra, the new peaks assigned to N 1s and Br 3d in PiP@QA comparing to HCP-OH (Fig. 1b vs. 1a) suggests that the quaternary ammonium bromide species have been successfully integrated into the porous skeleton of HCP-OH [27].

Nitrogen sorption isotherms collected at 77 K were measured to exam the porosity and specific surface area of HCP-OH and PiP@QA. As shown in Fig. 2, reversible type-I and IV isotherms were observed, which is typical for hierarchically porous materials. The steep nitrogen uptake at low relative pressure ( $P/P_0 < 0.01$ ) is due to the filling of the micropores, while the clear hysteresis loop is related to the small number of mesoporosity and macroporosity [31]. Brunauer–Emmett–Teller (BET) surface areas of HCP-OH and PiP@QA are 878 and 301 m<sup>2</sup>·g<sup>-1</sup>, respectively. Correspondingly, their pore sizes based on the nonlocal density functional theory (NLDFT) are mainly distributed at 1.4~2.1 nm and 0.6, 1.2~2 nm, respectively, which are consistent with their N<sub>2</sub> sorption isotherm results. Both  $S_{BET}$  and pore size of PiP@QA are obvious lower than that of HCP-OH, which is resulted from the occupation of pore space by the tetraalkylammonium cations together with counter anions [32, 33]. Notably, compared with some charged porous polymers, PiP@QA obtained through post-immobilization of ionic liquids exhibited satisfactory porous nature.

Figure 3 shows the field-emission scanning electron microscope (A, SEM) and transmission electron microscope (B, TEM) images of PiP@QA. It was found that this polymer was featured with the rough surfaces and abundant porosities [34]. The developed hierarchical porous channels could be beneficial for the enrichment of CO<sub>2</sub> molecules and the acceleration of mass transfer efficiency of reactants and products in the gas–liquid biphasic reaction system. The powder XRD pattern (Fig. 3c) shows no distinct characteristic diffraction peak, which further confirms the amorphous feature of PiP@QA.

Furthermore, considering of the existence of high charge density at the oxygen and nitrogen sites, the frameworks of

**Fig. 3** **a** SEM, **b** TEM images and **c** powder XRD pattern of PiP@QA

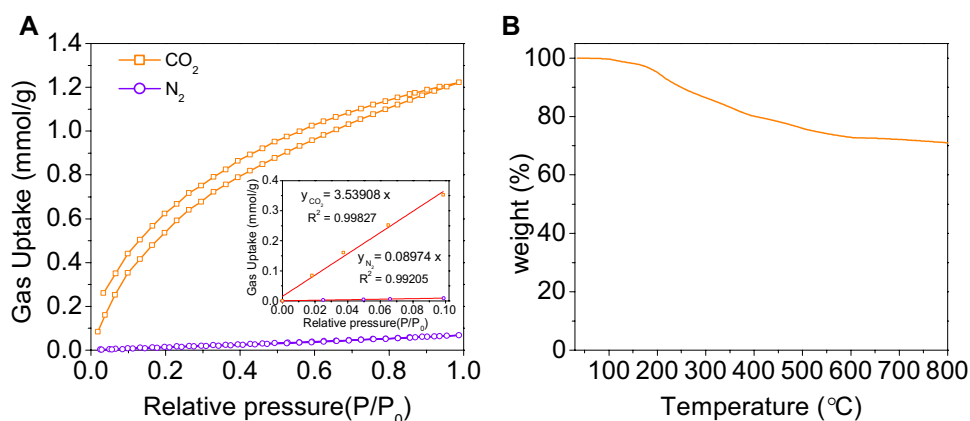


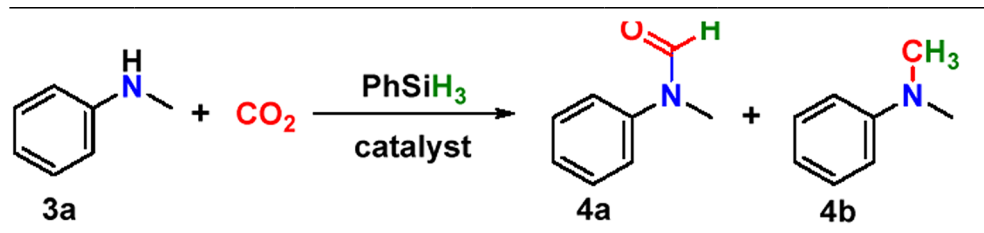
PiP@QA could provide stronger interaction towards CO<sub>2</sub> molecules [35, 36]. Hence, we collected the CO<sub>2</sub> isotherm at 298 K (Fig. 4a) for PiP@QA. Gratifyingly, PiP@QA presents a CO<sub>2</sub> uptake capacity of 1.22 mmol·g<sup>-1</sup> at 298 K and 1 bar, which is comparable to some other porous materials under the same conditions [37, 38]. The N<sub>2</sub> sorption capacity of PiP@QA was also measured at 298 K (Fig. 4a) and almost negligible N<sub>2</sub> uptake was observed under 1 bar. The selectivity for CO<sub>2</sub> over N<sub>2</sub> was calculated using Henry's Law constants by the ratios of the initial slopes of CO<sub>2</sub> and N<sub>2</sub> adsorption isotherms in the low pressure ( $P/P_0 < 0.1$  bar) range. As shown in Fig. 4a (inset), the CO<sub>2</sub>/N<sub>2</sub> selectivity of PiP@QA reaches to 39.4 at 298 K, which is superior to that of some POPs such as f TzTz-POP-1 (34) and TzTz-POP-2 (23) [39]. The above results indicate that PiP@QA possesses the selective adsorption ability for CO<sub>2</sub> in the CO<sub>2</sub>-N<sub>2</sub> coexistence system under atmosphere conditions, which is advantageous for using low concentration of CO<sub>2</sub> as building block for CO<sub>2</sub> cycloaddition reaction [40]. Additionally, the thermo gravimetric curve in Fig. 4b reveals that PiP@QA has good thermal stability with thermal degradation up to 200 °C.

### 3.3 Catalytic Evaluation

Initially, the catalytic activities of as-prepared polymeric catalysts were evaluated for the *N*-formylation reaction of *N*-methylaniline with CO<sub>2</sub> and PhSiH<sub>3</sub> under solvent-free conditions (Table 1). No conversion of *N*-methylaniline was observed at room temperature (35 °C) under 0.5 MPa CO<sub>2</sub> in the absence of any catalyst (Table 1, entry 1). The similar result was obtained by using HCP-OH as a catalyst under the same reaction conditions (Table 1, entry 2). The introduction of homogeneous quaternary ammonium bromide (QA), nearly quantitative conversion of *N*-methylaniline (1a) into *N*-methylformanilide (2a) was achieved (Table 1, entry 3), suggesting the quaternary ammonium bromide played pivotal role in this transformation. Encouragingly, the heterogeneous PiP@QA also presented excellent catalytic activity and chemoselectivity, which is comparable to the reported heterogeneous catalysts (Table S1). The high activity of PiP@QA could be explained as the enrichment of CO<sub>2</sub> molecules near the highly dispersed catalytic sites and the accelerated mass transfer of reactants and products originating from its nanopore structure and higher specific surface area.

**Fig. 4** **a** Gas adsorption isotherms of PiP@QA at 298 K (inset: the selectivity for CO<sub>2</sub> over N<sub>2</sub> obtained from the initial slope method); **b** Thermo gravimetric curve of PiP@QA under N<sub>2</sub> flow



**Table 1** Screening of the reaction conditions in the N-formylation reaction of *N*-methylaniline with CO<sub>2</sub> and PhSiH<sub>3</sub>


Entry	Catalyst	CO <sub>2</sub> (MPa)	T (°C)	t (h)	Conv. <sup>a</sup> (%)	Yield (%) <sup>a</sup>
1	– <sup>b</sup>	0.5	35	24	n.d. <sup>c</sup>	n.d
2	HCP-OH	0.5	35	24	n.d	n.d
3	QA	0.5	35	16	99	99
4	PiP@QA	0.5	35	16	99	99
5	PiP@QA	0.5	25	16	55	55
6 <sup>d</sup>	PiP@QA	0.5	35	16	67	67
7	PiP@QA	0.25	35	16	78	78
8	PiP@QA	0.1	25	54	71	70
9 <sup>e</sup>	PiP@QA	2.0	35	48	82	82

Reaction conditions: *N*-methylaniline (1.0 mmol), PhSiH<sub>3</sub> (1.0 mmol), catalyst (5.0 mol%, catalyst amount equal to the amount of Br)

<sup>a</sup>Yields of 4a (determined by GC using naphthalene as an internal standard)

<sup>b</sup>No catalyst

<sup>c</sup>Not detected

<sup>d</sup>Catalyst (2.5 mol%)

<sup>e</sup>Simulated flue gas (85% N<sub>2</sub>/15% CO<sub>2</sub>, v/v)

Whereas, the catalytic activity was strongly affected by reaction temperature, and only 55% yield of 2a was obtained at 25 °C (Table 1, entry 5). When the catalyst dosage decreased from 5.0 to 2.5 mol%, obvious decline in the yield of targeted product was observed (Table 4, entries 4 vs. 6). Surprisingly, PiP@QA retained far more than half of its original catalytic activity at half of CO<sub>2</sub> pressure (78% yield vs. 99% yield), which is well consistent with the inference about the advantages of large specific surface area and nanopore structure of PiP@QA [41]. It's more attractive to achieve the CO<sub>2</sub>-involved reaction under atmosphere at room temperature. PiP@QA could also efficiently catalyze N-formylation reaction of *N*-methylaniline with CO<sub>2</sub> to obtain 71% product yield under 0.1 MPa CO<sub>2</sub> at 25 °C by prolonging the reaction time to 54 h. Comparing with using high purity CO<sub>2</sub> as a feedstock, the direct use of flue gas in CO<sub>2</sub>-related reactions is surely more attractive. In light of the good CO<sub>2</sub> selective capture ability for PiP@QA, it is reasonable to study the catalytic performance of PiP@QA for direct transforming CO<sub>2</sub> in simulated flue gas (85% N<sub>2</sub>/15% CO<sub>2</sub>, v/v) into *N*-methylformanilide. As a result, an 82% yield of desired product was obtained at 35 °C under 2 MPa of CO<sub>2</sub>-N<sub>2</sub> gas mixture. Additionally, the effect of reaction time on *N*-methylformanilide yield was investigated and the corresponding kinetic curve was illustrated in Fig. 5a. With

the increase of reaction time from 0 to 14 h, the *N*-methylformanilide yield increased gradually at a higher rate. Then, the yield of product improved from 94 to 99% by prolonging the reaction time from 14 to 16 h.

The heterogenous PiP@QA catalyst could be easily recovered by filtration, washing with methanol/acetone and vacuum drying. Six-run recycling experiments for the N-formylation reaction of *N*-methylaniline with CO<sub>2</sub> were conducted to examine the recyclability and reusability of PiP@QA under the optimal reaction conditions for 8 h. Obviously, PiP@QA showed no significant loss in conversion and selectivity after six cycles (Fig. 5b). The quantitative leaching out of Br<sup>-</sup> was evaluated by oxygen flask combustion and mercury nitrate titration technique, which revealed 15.06 wt% Br in the recovered PiP@QA after six runs (15.13 wt% in fresh PiP@QA). Furthermore, the SEM image and N<sub>2</sub> adsorption isotherm of the reused catalyst clearly shows no apparent deterioration of the porous structure during the catalytic process (Fig. S1). These results demonstrate the good stability of PiP@QA as a robust heterogeneous catalyst for the chemical fixation of CO<sub>2</sub> at room temperature.

With the optimal reaction conditions in hand, the substrate scope was further expanded by using a series of secondary amines. Generally, as illustrated in Table 2, the newly developed N-formylation protocol proceeded with excellent

**Fig. 5** **a** Kinetic curve for N-formylation of CO<sub>2</sub> with N-methylaniline catalyzed by PiP@QA (Reaction conditions: N-methylaniline 1.0 mmol, PhSiH<sub>3</sub> 1.0 mmol, catalyst 5.0 mol%, 35 °C, CO<sub>2</sub> 0.5 MPa); **b** recyclability test of PiP@QA (Reaction conditions: N-methylaniline 1.0 mmol, PhSiH<sub>3</sub> 1.0 mmol, catalyst 5.0 mol%, 35 °C, CO<sub>2</sub> 0.5 MPa, 8 h)

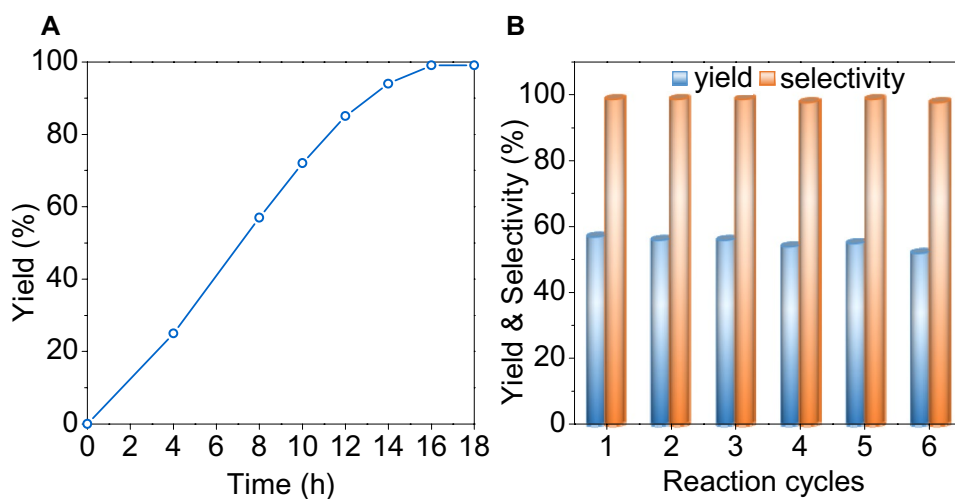
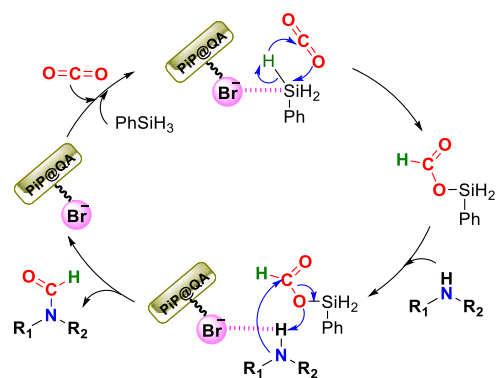


**Table 2** N-formylation of CO<sub>2</sub> with various amines catalyzed by PiP@QA

1		6	
2		7	
3		8	
4		9	
5		10	

<sup>a</sup> Reaction conditions: amine (1.0 mmol), PhSiH<sub>3</sub> (1.0 mmol), catalyst (5.0 mol%, catalyst amount equal to the amount of Br), 0.5 MPa, 24 h. <sup>b</sup> Yields of formamides.

catalytic reactivity and selectivity. Various substituents in the aromatic amine substrate including methoxy (2), methyl (3), and chloro (4) groups were tolerated, and electron-donating groups could give the higher activity (entries 2, 3 vs. 4). Obviously, the amines bearing larger steric hindrance substituent also turned out to be more challenging substrates (entries 6 vs. 5 and 1). Pleasingly, for aliphatic amine derivatives, outstanding catalytic performance was also achieved when these substrates bearing either alkyl chain or heterocyclic groups were used (entries 7–10). Notably, all the above catalytic experiments gave no byproduct, which indicated their significant chemselectivity in this catalytic system.



**Scheme 2** Proposed reaction mechanism for the N-formylation of amines with CO<sub>2</sub> and PhSiH<sub>3</sub> over PiP@QA

### 3.4 Proposed Mechanism

Based on the above catalytic results and in combination with previous works [30, 33], the proposed reaction mechanism for the N-formylation of amine with CO<sub>2</sub> and PhSiH<sub>3</sub> over PiP@QA was deduced as described in Scheme 2. The Si–H bond in PhSiH<sub>3</sub> was first activated by Br<sup>−</sup> in the catalyst PiP@QA. The enriched CO<sub>2</sub> molecule in the porous channel was then inserted into the activated Si–H bond, affording a highly active pivotal silyl formate intermediate. Meanwhile, the coordination occurred between Br<sup>−</sup> of PiP@QA and the H atom of secondary amino group in amine through intermolecular hydrogen bonding to form an activated substrate containing a nucleophilic nitrogen atom. Subsequently, a new C–N bond formed through a nucleophilic attack of nitrogen atom on the electron-deficient carbon atom of silyl formate intermediate, thus producing the final targeted formamide.

## 4 Conclusions

In summary, we reported here a heterogeneous porous ionic polymer catalyst (PiP@QA) that was synthesized from the Friedel–Crafts alkylation reaction of 1,1'-bi-2-naphthol with formaldehyde dimethyl acetal and subsequent Williamson ether reaction with quaternary ammonium bromide. We have demonstrated that the PiP@QA presented improved specific surface area, hierarchical porosity, CO<sub>2</sub> absorbability and selectivity, as well as open charged species. Its inherent CO<sub>2</sub> enrichment ability, well-defined nanopores and exposed ionic sites allow this PiP@QA to promote effective reduction of captured CO<sub>2</sub> with wide-scope amines and phenylsilane at room temperature in the absence of solvent. PiP@QA is easy-to-recovering and has been demonstrated to retain complete catalytic activity and selectivity for over six runs. Moreover, PiP@QA exhibits high efficiency for the selective conversion of diluted CO<sub>2</sub> (15% CO<sub>2</sub> in N<sub>2</sub>, v/v) under mild conditions. Our strategy will facilitate the development of PiPs and their application as robust platforms for efficient utilization of C1 resources.

**Supplementary Information** The online version of this article (<https://doi.org/10.1007/s10562-020-03527-y>) contains supplementary material, which is available to authorized users.

**Acknowledgements** We gratefully acknowledge the financial support from the National Natural Science Foundation of China (21938001, 21961160741 and 22078072), the Guangdong Basic and Applied Basic Research Foundation (2019A1515010612), the Natural Science Foundation of Guangdong Province (2018A030307004), Characteristic Innovation Project of Guangdong Ordinary University (2019KTSCX107), Guangdong University of Petrochemical Technology Scientific Research Foundation (2019rc049), Local Innovative and Research Teams Project of Guangdong Pearl River Talents Program (2017BT01C102), Innovation Team Project of Guangdong Ordinary University (2019KCXTD002) and Scientific Research Innovation Team Foundation of Guangdong University of Petrochemical Technology.

## Compliance with Ethical Standards

**Conflict of interest** There are no conflicts to declare.

## References

- Das Neves Gomes C, Jacquet O, Villiers C, Thuéry P, Ephritikhine M, Cantat T (2012) *Angew Chem Int Ed* 51:187
- Liu Q, Wu LP, Jackstell R, Beller M (2015) *Nat Commun* 6:5933
- Yuan GQ, Qi CR, Wu WQ, Jiang HF (2017) *Curr Opin Green Sust Chem* 3:22
- Liu X-F, Ma R, Qiao C, Cao H, He L-N (2016) *Chem Eur J* 22:16489
- Hao L, Zhao Y, Yu B, Yang Z, Zhang H, Han B, Gao X, Liu Z (2015) *ACS Catal* 5:4989
- Saptal V, Shinde DB, Banerjee R, Bhanage BM (2016) *Catal Sci Technol* 6:6152
- Jacquet O, Das Neves Gomes C, Ephritikhine M, Cantat T (2012) *J Am Chem Soc* 134:2934
- Xie C, Song J, Wu H, Zhou B, Wu C, Han B (2017) *ACS Sustainable Chem Eng* 5:7086
- Fang C, Lu C, Liu M, Zhu Y, Fu Y, Lin B-L (2016) *ACS Catal* 6:7876
- Wang M-Y, Wang N, Liu X-F, Qiao C, He L-N (2018) *Green Chem* 20:1564
- Li XF, Zhang XG, Chen F, Zhang XH (2018) *J Org Chem* 83:12815
- Frogneux X, Jacquet O, Cantat T (2014) *Catal Sci Technol* 4:1529
- Riduan SN, Ying JY, Zhang Y (2016) *J Catal* 343:46
- Zhou H, Wang G-X, Zhang W-Z, Lu X-B (2015) *ACS Catal* 5:6773
- Chong CC, Kinjo R (2015) *Angew Chem Int Ed* 54:12116
- Zhao WF, Chi XP, Li H, He J, Long JX, Xu YF, Yang S (2019) *Green Chem* 21:567
- Liu X-F, Li X-Y, Qiao C, Fu H-C, He L-N (2017) *Angew Chem Int Ed* 56:7425
- Hulla M, Ortiz D, Katsyuba S, Vasilyev D, Dyson PJ (2019) *Chem Eur J* 25:11074
- Luo RC, Lin XW, Lu J, Zhou XT, Ji HB (2017) *Chin J Catal* 38:1382
- Liu Z-W, Han B-H (2019) *Curr Opin Green Sust Chem* 16:20
- Sun Q, Jin Y, Aguila B, Meng X, Ma S, Xiao F-S (2016) *ChemSuschem* 10:1160
- Chen Y, Luo R, Ren Q, Zhou X, Ji H (2020) *Ind Eng Chem Res* 59:20269
- Hui W, He X-M, Xu X-Y, Chen Y-M, Zhou Y, Li Z-M, Zhang L, Tao D-J (2020) *J CO<sub>2</sub> Util* 36:169
- Song Y, Sun Q, Aguila B, Ma S (2020) *Catal Today* 356:557
- Song Y, Sun Q, Lan PC, Ma S (2020) *ACS Appl Mater Interfaces* 12:32827
- Xu D, Guo JN, Yan F (2018) *Prog Polym Sci* 79:121
- Chen YJ, Luo R, Xu QH, Jiang J, Zhou XT, Ji HB (2018) *ACS Sustainable Chem Eng* 6:1074
- Li J, Jia DG, Guo ZJ, Liu YQ, Lu YN, Zhou Y, Wang J (2017) *Green Chem* 19:2675
- Huang K, Zhang J-Y, Liu FJ, Dai S (2018) *ACS Catal* 8:9079
- Chen YJ, Luo RC, Bao JH, Xu QH, Jiang J, Zhou XT, Ji HB (2018) *J Mater Chem A* 6:9172
- Dai ZF, Sun Q, Liu XL, Bian CQ, Wu QM, Pan SX, Wang L, Meng XJ, Deng F, Xiao F-S (2016) *J Catal* 338:202
- Sun Q, Aguila B, Perman J, Nguyen N, Ma S (2016) *J Am Chem Soc* 138:5790
- Dong B, Wang L, Zhao S, Ge R, Song X, Wang Y, Gao Y (2016) *Chem Commun* 52:7082
- Chen YJ, Luo RC, Xu QH, Jiang J, Zhou XT, Ji HB (2017) *ChemSuschem* 10:2534
- Zhu J-H, Chen Q, Sui Z-Y, Pan L, Yu J, Han B-H (2014) *J Mater Chem A* 2:16181
- Dani A, Crocellà V, Magistris C, Santoro V, Yuan J, Bordiga S (2017) *J Mater Chem A* 5:372
- Xie YQ, Sun Q, Fu YW, Song L, Liang J, Xu X, Wang HT, Li JH, Tu S, Lu X, Li J (2017) *J Mater Chem A* 5:25594
- Li J, Han YL, Ji T, Wu NH, Lin H, Jiang J, Zhu JH (2019) *Ind Eng Chem Res* 59:676
- Zhu X, Tian C, Jin T, Wang J, Mahurin SM, Mei W, Xiong Y, Hu J, Feng X, Liu H, Dai S (2014) *Chem Commun* 50:15055
- Chen J, Li H, Zhong MM, Hua YQ (2016) *Green Chem* 18:6493
- Wang JQ, Sng WH, Yi GS, Zhang YG (2015) *Chem Commun* 51:12076

**Publisher's Note** Springer Nature remains neutral with regard to jurisdictional claims in published maps and institutional affiliations.

## Authors and Affiliations

Qinggong Ren<sup>1</sup> · Yaju Chen<sup>1</sup> · Yongjian Qiu<sup>1,2</sup> · Leiming Tao<sup>1</sup> · Hongbing Ji<sup>1,2,3</sup>

<sup>1</sup> School of Materials Science and Engineering, Guangdong University of Petrochemical Technology, Maoming 525000, People's Republic of China

<sup>2</sup> School of Chemistry and Chemical Engineering, Guangxi University, Nanning 530004, People's Republic of China

<sup>3</sup> Fine Chemical Industry Research Institute, School of Chemistry, Sun Yat-Sen University, Guangzhou 510275, People's Republic of China